# THE INTERPRETATION OF ANOMALOUS FIELDS BY USING THEIR FREQUENCY CHARACTERISTICS

## I.I. ROKITYANSKY*

*Academy of Sciences Ukranian S.S.R., Institute of Geophysics, Kiev (U.S.S.R.)*

Non-synoptic small array studies for magnetometer-induction investigations are considered. A new interpretation technique based on the fact that anomalous fields originate from current concentrations in local inhomogeneities is discussed. Two-dimensional and three-dimensional inhomogeneities are considered and results from some analogue modelling measurements are also described. The determination of various parameters associated with the anomalies is discussed.

## 1. Introduction

Magnetometer induction investigations may be divided into two types: (a) "array studies" and (b) "non-synoptic small array studies". The term "array study" implies the performance of synchronous observations in the area under investigation with special data processing and interpretation of synchronous variations recorded in the area.

A "non-synoptic small array study" includes point observations and profile synchronous observations. Earlier electrical conductivity anomalies were studied only by point and profile observations and therefore such non-synoptic small array studies may be considered classical. The coast effect as well as the northern Germany, Japanese, Andean, Alert, Carpathian, Kyro-vograd and other anomalies were detected and studied by this method.

The data processing technique for point and profile observations is well developed and was presented in the review by Banks at the Edinburgh Workshop (Banks, 1973). Therefore, little attention will be paid to this question in the present review. The technique for interpretation of the anomalous fields is not well developed. Much of this review is devoted to a new interpretation technique that is based on the fact that anomalous fields originate due to the conductive current concentration in local inhomogeneities. As the basis of this technique, the analysis of a large set of two-dimensional numerical solutions (insertion and graben) and deep inhomogeneities (elliptical cylinders) is carried out. Physical modelling of bodies of limited length has also been done.

Finally, the technique of quantitative interpretation of anomalous fields is presented, and the possibilities of the MVP (MVP = GDS) method are described. The published data on the frequency characteristics of the coast effect are analyzed and conclusions about the parameters of its source are derived.

## 2. The integral relations between anomalous field components

The normalized anomalous fields from two-dimensional inhomogeneities elongated along the $y$ axis satisfy the Hilbert transformations (Kertz, 1954; Schmucker, 1970):

$$h_x(x_0) = -Kh_z(x), \qquad h_z(x_0) = Kh_x(x) \tag{1}$$

where

$$Kh(x) = -\frac{1}{\pi} \cdot \int_{-\infty}^{\infty} \frac{h(x)}{x - x_0} dx, \qquad h_x = \frac{H_{xa}}{H_{x0}},$$

$$h_z = \frac{H_{za}}{H_{x0}}$$

If the anomalous fields from the observational data satisfy eq. 1, then the profiles may be interpreted according to two-dimensional models. All $h_r$ ($r = x,z$) values in eq. 1 are complex amplitudes, the real ($h_{ru}$) and imaginary ($h_{rv}$) parts of which are also connected by the Hilbert transformation (Kaufman, 1960):

$$h_{ru}(T_0) = Kh_{rv}(T), \qquad h_{rv}(T_0) = -Kh_{ru}(T) \qquad (2)$$

where

$$Kh(T) = -\frac{1}{\pi} \int_{-\infty}^{\infty} \frac{h(T)}{\log T - \log T_0} d(\log T)$$

and where $T$ is the period. Similarly, the logarithm of the amplitude of the field is related by a Hilbert transform to its phase.

The relations (1) and (2) show that if the real or imaginary part of one of the anomalous field components is given in the whole $(x,T)$ domain, then the anomalous field is defined completely and its other components may be computed by the integral transformations (1) and (2). It follows that measurement of only one (e.g., $h_{ru}$) or two components of the anomalous field is not a major drawback in limiting the interpretation. However, this does not mean that measuring only one component is advisable. In practice the observations are always limited in frequency and space by separate points where every component of the anomalous field is measured with some error. In such conditions it is desirable that various components should be observed as this gives more information and also increases the accuracy of the information received provided that the measurement accuracy of the various components is comparable. In practice the normalized anomalous field may be obtained either as the result of processing profile synchronous observations or from observations at each point independently. In the former case the processing results are transfer functions $h_{iK}(x,y,T)$ (Schmucker, 1970; Banks, 1973), that form the matrix. In the latter case

the processing results are the combination of these functions that define the induction vector $C$. For a two-dimensional anomaly elongated along the $y$ axis:

$$|C| = C_x \simeq \frac{h_z}{1 + h_x} (x,T) \qquad (3)$$

Analytical methods have been developed for calculating $h_x$ and $h_z$. If processing is done for each point independently, it is possible to calculate approximately $h_z$ from $C_x$ by making some assumptions about the anomaly.

## 3. Two-dimensional models

### 3.1. Anomalous fields of two-dimensional inhomogeneities

The solution of the problem of electromagnetic induction in a heterogeneous earth by ionospheric or magnetospheric sources of complex configuration is the basis for data interpretation. Such a problem is extremely complex mathematically, and also the source is highly variable and its parameters may be only approximately known. Considerable difficulties may be avoided if the problem is separated into two simpler ones: (1) The formation of large-scale normal magneto-telluric fields ($E_0,H_0$) corresponding to the configuration and dimensions of the source in some appropriate horizontally-stratified Earth; and (2) the formation of anomalous fields by the local inhomogeneity under the action of $E_0$ and $H_0$. The smaller the dimensions of the electrical conductivity anomaly as compared to the source dimensions the better the results given by such a division.

The former problem is solved for a number of source models. For most real sources the impedance on the Earth's surface is close to the impedance for a vertically incident plane wave (Rokityansky, 1972). It is difficult to analyze possible deviations of real variations from this rule (array studies over large areas are required) so that, at present, the plane-wave model is used for local studies. Analysis of the role of the vertical component of the normal field in the formation of the anomalous field of a local inhomogeneity justifies the adopted model. The impedance $\zeta_0 = E_0/H_0$ will then be the only important characteristic (except for period and polarization) of the normal field. The nor-

mal continental impedance for various surface conditions characterized by $S$ were presented by Rokityansky (1972, 1974). Next, the solution of the latter problem is considered, that is, the anomalous field formation by local inhomogeneities in the field of a plane wave for $E$-polarization (the anomalous field for $H$-polarization is equal to zero at the surface of the conducting half-space).

### 3.2. Two-dimensional surface inhomogeneities — Insertion and graben

This problem is solved by the integral equation method and numerical results are obtained for inhomogeneities with a wide set of parameters (Dmitriev and Kokotushkin, 1971; Dmitriev et al., 1973). The period interval $(T_0 - \Delta T/2, T_0 + \Delta T/2)$ where the anomalous field amplitude exceeds 0.5 of its maximum value will be referred to as the central part of the frequency dependence. In this interval the phase passes through zero at some period $T_{0\phi}$. Usually $T_{0\phi} \simeq T_M \simeq \simeq T_0$ where $T_M$ is the position of the maximum of the amplitude curve. Analysis of the numerical results for insertions shows that the central and long-period parts of the amplitude curves are similar and the phase curves coincide for both components of anomalous field at all points where these components are large. This fact is of great importance because it shows the stability of the determination of the two-dimensional anomalous body parameters by the frequency dependences regardless of the observation point (including the singular point at the contact). Comparative analysis of anomalous fields of an insertion and a similar graben shows that their fields at central and long periods are almost identical at all profile points and even at the contact the difference does not exceed 10%. Thus for the central frequencies the insertion and graben models are practically identical and it is not necessary to analyze the graben model especially, but the results obtained for insertions may also be used for grabens and probably for a large class of elongated surface inhomogeneities.

At short periods $(T \ll T_0)$ the amplitude and phase of an anomalous field strongly depend on the observation point and differ between insertion and graben for horizontal and vertical components. The curves at these periods do not appear to contain information

on the anomalous body as a whole but on the nearest parts of its section.

The analysis of the insertion (Fig. 1A) with $\sigma_i/\sigma_e$ = 5, 10, 16 and $2L/h < 10$ ratios gives the same result. For thin insertions $(2L/h > 10)$ the curves in the central part of the frequency range at various observation points are distorted due to the horizontal skin-effect influence.

The influence of the depth $H$ to the ideally conducting basement on $h_z$ is presented in Fig. 1B. This figure shows that the position of the maximum in the amplitude curve and the position of the sign change in the phase curve do not characterize uniquely the longitudinal conductivity of the anomalous body $(2Lh\sigma_i)$, but depend on $H$, i.e. on the deep geoelectrical structure. characterized by the normal impedance $\zeta_0$.

Fig. 1C presents the impedance $\zeta_0$ of the normal three-layered section $1/\rho = \sigma_e, 0, \infty; h = I, H, \infty$ (see Fig. 1A) with $H$ values corresponding to the curves in Fig. 1B. The similarity of $h_z$ and $\zeta_0$ at long periods in Figs. 1B and 1C indicates the existence of a linear relation between them, which indicates an electrical- or conductive-type anomaly. Introducing a function $V$ which denotes the frequency dependence $h_z/E_0$ in a similar way to the formula for a cylinder (Rokityansky et al., 1969; Rokityansky, 1972, 1974) and by normalizing such that $V \xrightarrow{T \to \infty} I$, we can write:

$$h_r = V\zeta_0 S_0 h_{r,\infty} \qquad r = x,z \qquad (4)$$

where $S_0 = \sigma_e h$ is the longitudinal conductivity of the upper layer outside the insertion and the constant $h_{r,\infty} = \lim h_r$ as $T \to \infty$ and $H \to \infty$.

Validity of eq. 4 will be confirmed if the value $V = h_r/(S_0 h_{r,\infty} \zeta_0)$ does not depend on $H$. Fig. 1D presents the results of such a determination for six insertions. Function $V$ determined on the curves $H = 51.125$ and $\infty$ coincides in the range of plotting accuracy (2—3%). The determined value of $V$ for the curves $H = 21$ is presented for three insertions by crosses. The deviation of crosses from the curve, obtained at higher $H$, shows that at $H = 21$ the anomalous current interaction in the insertion with currents in the conducting basement is quite noticeable in a definite period interval. At longer or shorter periods this interaction is less because one of the interaction currents becomes small. With the increasing insertion width the interaction increases and its maximum influence
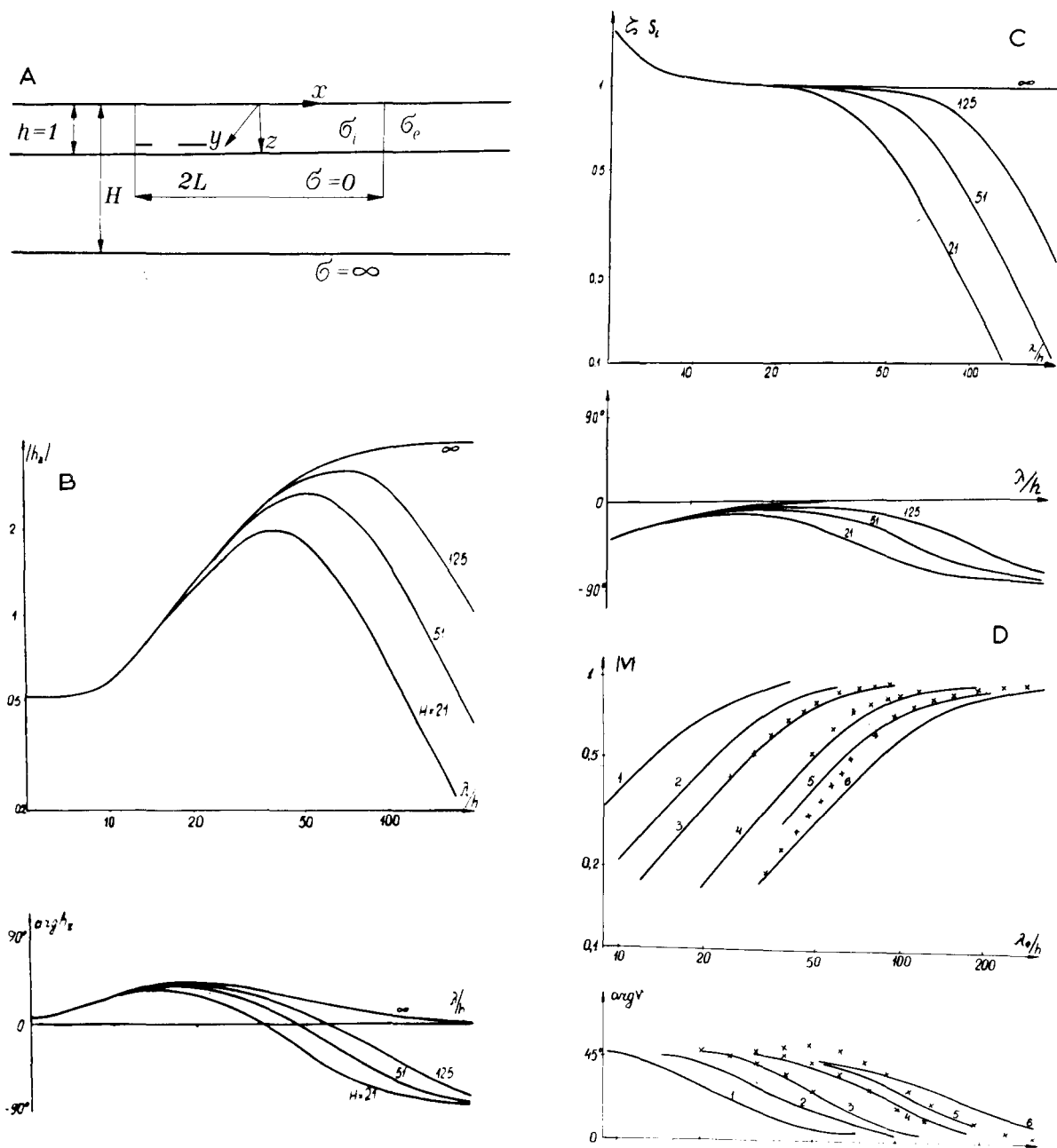
Fig. 1. The anomalous field frequency dependence for the insertion at point $x = L$.

A. Cross-section of the model.

B. For different $H$, $\sigma_i/\sigma_e = 16$, $L = 1$.

C. Normal impedance multiplied by $S_0 = \sigma_e \cdot h$.

D. The function $V = h_z/S_0 s_0 h_{z\infty}$ for six insertions (see table below). Crosses are the results of calculations for the cases 3, 4, 6 with $H = 21$. The distance from the crosses to the corresponding solid curves characterizes the effect of the interaction of the anomalous currents with the conducting basement currents.

| Curve number | $\sigma_i/\sigma_e$ | $L$ | $h_{z\infty}$ | Curve number | $\sigma_i/\sigma_e$ | $L$ | $h_{z\infty}$ |
|---|---|---|---|---|---|---|---|
| 1 | 5 | 1 | 1.55 | 4 | 16 | 2.5 | 5.8 |
| 2 | 10 | 1 | 2.4 | 5 | 16 | 4 | 7.0 |
| 3 | 16 | 1 | 4 | 6 | 16 | 8 | 8.5 |

on the anomalous field at $H = 21$ is 6% at $L = 1$, 11% at $L = 2.5$, 20% at $L = 4$ and 30% at $L = 8$.

Generalizing these data it is found that the interaction of the anomalous currents due to the insertion with currents in the conducting basement changes the anomalous field less than 5% at $2L/H < 0.1$ and less than 10% at $2L/H < 0.2$. The conducting basement is at a depth of more than 400 km, and so for anomalies of 80 km width the frequency dependence may be synthesized with less than 10% error by multiplying the function $V$ by the impedance of the normal section, that is formula (4) may be used. Using global continental data as the normal impedance $\zeta_0$ (Rokityansky, 1972, 1974), the frequency dependence for a large set of insertions was plotted.

### 3.3. Deep anomalies

The analytical solution for an external anomalous field of a circular cylinder with radius $a$ and conductivity $\sigma_i$ in the field of a plane $E$-polarized wave has the form:

$$\begin{pmatrix} H_{ra} \\ H_{\phi a} \\ H_{za} \end{pmatrix} = -\frac{1}{2} E_{0h}\sigma_i V\left(k_i a, \frac{\sigma_i}{\sigma_e}\right)\frac{a^2}{r}\begin{pmatrix} 0 \\ 1 \\ 0 \end{pmatrix} -$$

$$- H_{0h}D(k_i a)\frac{a^2}{r^2}\begin{pmatrix} \sin\phi \\ \cos\phi \\ 0 \end{pmatrix} \qquad (5)$$

where $k_i = (i\omega\mu\sigma_i)^{1/2}$. $V$ is a limited monotonously increasing function $|V| < 1$ and $D$ is a monotonously decreasing function of period. The first term in eq. 5 corresponds to a conductive-type anomaly, and the second term to an eddy-type anomaly.

Conductive anomalies are due to the current redistribution between the medium and the body (which is more evident for a conductor of limited length). Such anomalies are proportional to $E$ and therefore to the impedance $\zeta_0$. On the basis of eq. 5 it is possible to write a generalized formula for the fields of conductive nature (Rokityansky et al. 1969; Rokityansky, 1972, 1974):

$$h(T,r) = A(r)V(T)\beta(T,r)\zeta_0(T) \qquad (6)$$

where $\beta(T,r)$ is a function which expresses damping in the enclosing medium and $V(T)$ is a function which

determines the degree of saturation of anomalous currents by the conductor. 100% saturation refers to the case when the electric field is the same in the conductor and in the surrounding medium. Calculation of the functions $\zeta_0$, $V$, and $\beta$ gives the approximate frequency dependence of a conductive-type anomalous field. If $\zeta_0(T)$ and $\beta(T)$ are known, then according to the observed frequency dependence of $h(T)$, $V(T)$ can be determined. Comparing the latter with the theoretical curve $V(1/k_i a)$ (Svetov, 1966, 1973; Rokityansky, 1972) and considering their horizontal shift, $G = \pi a^2 \sigma_i$ may be determined.

The second term of eq. 5 gives a magnetic- or eddy-type anomaly which is proportional to $H_0$ and does not depend on the conductivity of the surrounding medium and shows little dependence on the conductor elongation. Our estimates show that for local inhomogeneities (where the anomaly width is much less than the characteristic dimensions of the source field) in real geophysical conditions the eddy anomaly is usually small even though the whole internal field of the geomagnetic variations is of eddy nature. This is confirmed by the analysis of numerical solutions for surface inhomogeneities (Section 3.2) and will also be confirmed by the analysis of numerical results for deep anomalies in the next section.

### 3.4. Deep two-dimensional anomalies – The elliptical cylinder (Fig. 3C)

The calculation methods and the analysis of results of the solution for the problem of a plane-wave electromagnetic field incident on a medium containing an elliptical cylinder ($E$-polarization) are described in the work by Kaufman et al. (1971a) and an album of master curves of $h_x$, $E_y$ and $\rho_a$ as a function of period has been published by Kaufman et al. (1971b). Important results from these works are referred to here.

Functions $V$ (Fig. 2) are determined by using the normal impedance for a half-space and the anomalous field frequency dependence of a set of elliptical cylinders with $z/b = 3$. Values of $V$, calculated for cylinders both with and without a surface conducting layer were practically the same at long and intermediate periods. This shows that the anomalous field weakening at periods satisfying the condition $\lambda_1 > 10 \cdot h_1$ is due primarily to electrical field attenuation proportional to $\zeta_0$. An important result from this
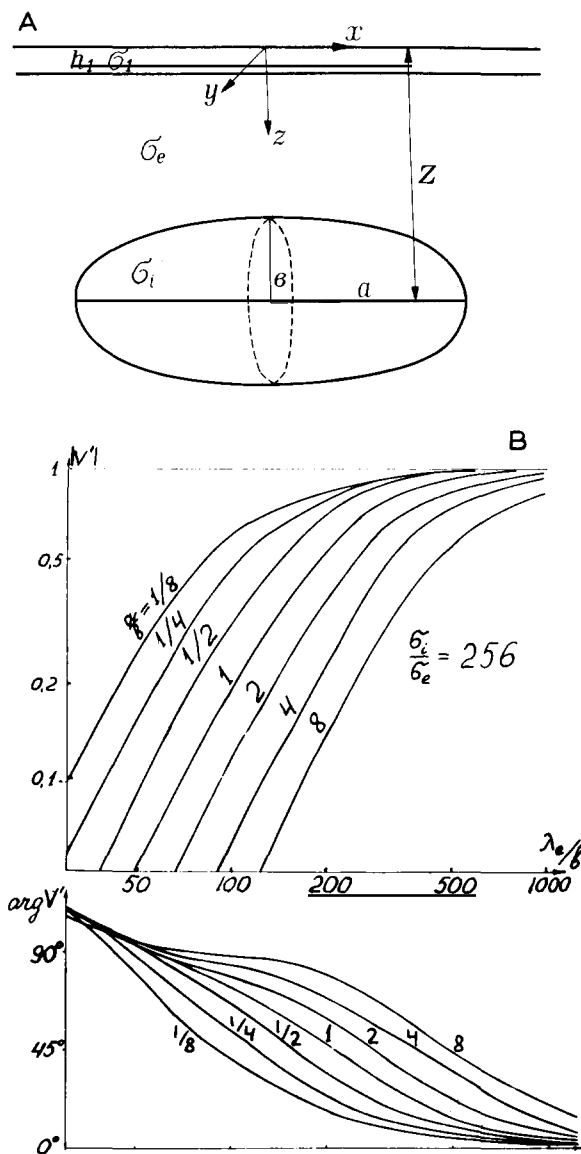
Fig. 2. The frequency dependence of the function $V$ for elliptical cylinders with different $a/b$.
A. Cross-section of the model.
B. Dependence for $\sigma_i/\sigma_e = 256$.

is that $V$ may be calculated from $h_x$ or $h_z$ according to formula (6) even for the case of a conducting layer over the anomalous body if $\lambda_1 > 10 \cdot h_1$.

The frequency dependences synthesized according to formula (6) by multiplying the function $V(\lambda_e/b)$ (Fig. 2) for elliptical cylinders by the normal impedance $\zeta_0(T)$ show how the surface conducting layer weakens

the anomalous field at high frequencies. As $S$ increases, the weakening spreads over the central part of the frequency curve and shifts the maximum to the right as well as reduces its level. Under these conditions the anomaly is screened. If an anomalous field from a deep object is not completely screened and is measurable at the surface, then by knowing the parameters of the surface layer it is possible to approximate its influence and determine the frequency and space distribution of the anomalous field from the deep anomaly being studied.

### 3.5. Comparison of the surface and deep anomalies

Comparison of the synthesized frequency dependences according to formulae (4) and (6) shows that both the amplitude and phase curves for surface and deep anomalies (insertion and elliptical cylinder) have practically the same form at central and long periods. At short periods the field associated with the elliptical cylinder becomes smaller more quickly than that due to the insertion. However, if the observation point is not chosen at the insertion edge no difference appears. Considering that real surface inhomogeneities have smoother slopes than the vertical contact of the insertion model one may conclude that it is impossible to distinguish deep anomalies from surface ones according to the frequency dependence for both amplitude and phase. It is also impossible to do this by considering the form of the profile curves. The differences observed at short periods cannot be used to determine the basic anomaly depth because they may be connected with the existence of smaller-scale electrical conductivity inhomogeneities.

### 4. Three-dimensional models

Two-dimensional considerations are always idealized and even to show the limits of their applicability the analysis of three-dimensional solutions is required. Existing solutions for continuous current (Svetov, 1966, 1973; Rokityansky and Shuman, 1970) cannot help one to find the frequency dependencies of a conductive-type anomalous field. The analytical solution of the diffraction problem is known for a sphere only. It is insufficient, however, for the interpretation of observed anomalies because simple considerations show
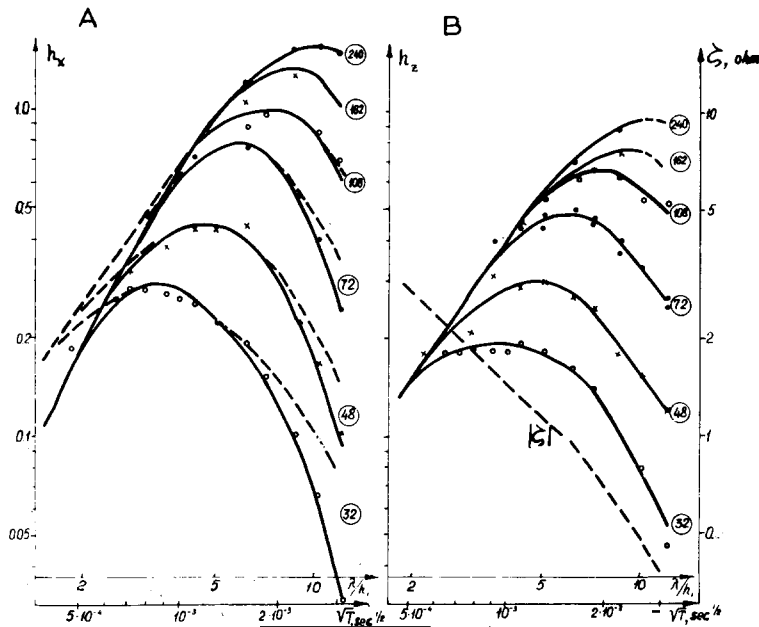
Fig. 3. The anomalous field frequency dependence over a horizontal brass plate of $1.5 \cdot 10^{-4} \times 0.02$ km section and length $L_y$ (m$^2$) indicated by the large circles. Points, crosses and circles are the experimental data for plates of different length. Solid lines are smoothed experimental data.

A. $h_x^* = (|H_x| - |H_{x0}|)/H_{x0}$. The dashed line is $|h_x|$ according to eq. 2 with the assumption $h_x^* \simeq \mathrm{Re}\, h_x$.

B. $h_z = H_z/H_{x0}$. The dashed line is the impedance on the two-layered section: $\rho_1 = 0.24$ $\Omega$m, $h = 0.405$ m, $\rho_2 = 0$. $\lambda/h$ on the absciss-axis for $h = 0.405$ m.

that a conductive anomaly depends essentially on the anomalous body elongation along the electric-field direction. The influence of elongation was studied by modelling experiments in a tank (Rokityansky and Kulick, 1972). Fig. 3 shows the obtained frequency dependence of $h_x$ and $h_z$ of the anomalous field for bodies of different length. The fact that the anomalous field observed in the model is of conductive nature is confirmed by the following features: dependence on the length, similarity of the long period dependence on the normal section impedance $\zeta_0$ (Fig. 3B), and the anomalous field exhibited for different profiles, in particular, outside the body edges.

The analysis of two limiting formulae for an elongated spheroid in a continuous current (Rokityansky, 1972; Svetov, 1966, 1973) and eqs. 5 and 6 for a cylinder make it possible to assume eq. 6 to describe the modelling results, where $V^*$ should be substituted for $V$ defined by the expression:

$$\frac{1}{V^*} = \frac{1}{V} + \frac{\sigma_i}{\sigma_e} \frac{\chi}{2} \tag{7}$$

$\chi$ is a function which decreases sharply as the body becomes more elongated (Svetov, 1966, 1973) as shown in the table:

| $2L_y/(L_x+L_z)$ | 2 | 10 | 50 | 200 |
|---|---|---|---|---|
| $\chi$ | 0.4 | 0.04 | 0.003 | 0.0003 |

If the first term on the right hand side of eq. 7 dominates $(1/V \gg \sigma_i\chi/2\sigma_e)$ the limiting formula for a cylindrical inhomogeneity is obtained. If the second term dominates $(1/V \ll \sigma_i\chi/2\sigma_e)$ a spherical-type conductor exists (Svetov, 1966, 1973; Rokityansky, 1972) and the anomalous field for it is determined by the enclosing medium conductivity $\sigma_e$ and by the body elongation. The solutions obtained for continuous currents are applied to a spherical-type conductor, and the frequency dependence is determined by calculation of $\beta\zeta_0$ according to eqs. 6 and 7. When the terms on the right side of eq. 7 are comparable in value, the expression (7) should be regarded as an empirical one.

The results described above are for the central profile across the elongated body. With the observations

approaching the body edges the anomalous field de-
creases at long periods and the maximum shifts to the
short-period range. The same occurs for the central
profile when the body length is reduced.

Fig. 4 presents the frequency dependence (synthe-
sized according to eqs. 6 and 7) of the conductive-type
anomalous field over a spheroid of different elongation
$2L_y/(L_x + L_z)$ where $E_0$ is parallel to the major dimen-
sion $L_y$. The eddy anomaly depends little on elonga-
tion (in Fig. 4 it is plotted as a dashed line for the
sphere and cylinder). At long periods the conductive
anomaly sharply decreases as the elongation decreas-
es, and the maximum shifts to the short-period range.
In the central part of the curve with $2L_y/(L_x + L_z)$
< 3 the eddy anomaly exceeds the conductive one
for a body of given parameters, and the anomalous
field value is practically unmeasurable because the
anomalous field background from the subsurface
objects is greater than 0.1–0.2.

Fig. 4 shows that by using eqs. 6 and 7 and con-
sidering the frequency dependence of the anomalous
field it is possible within the framework of the
spheroid model to estimate the minimum length of
the anomalous body if reasonable assumptions are
made for the conductivities $\sigma_e$ and $\sigma_i$.
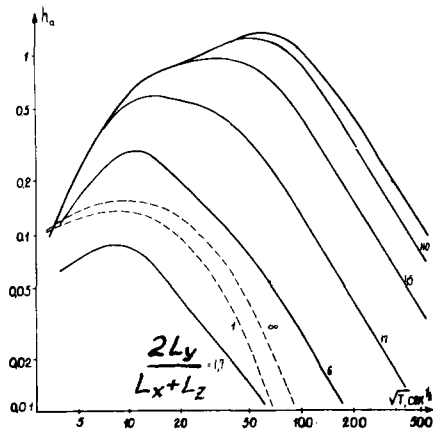


Fig. 4. The anomalous field of a conductive nature (solid lines)
synthesized according to the formulae (6) and (7) using normal
global impedance (Rokityansky, 1972, 1974) for the spheroids
with different elongation $2L_y/(L_x + L_z)$. The dashed lines are
the eddy field. Parameters of the model: the radius of the
equatorial section $L_x = L_z = a = 20$ km, $\sigma_e = 10^{-3}$ $\Omega^{-1}$ $m^{-1}$, $\sigma_i$
= 1 $\Omega^{-1}$ $m^{-1}$, $z = 2a$.

## 5. The anomalous field interpretation

### 5.1. The non-uniqueness of the inverse problem

In practice the MVP inverse problem does not
give a single-valued solution. This fact has not been
given due attention and the interpretation results
have usually been presented in the form of a random
model. The purpose of MVP interpretation is the
determination of the whole set of models satisfying
the experimental data which, for example, can be
carried out by the limiting estimation method.

The next interpretation step includes the use of
other geoelectrical method data. The first of these
is the MTS in order to narrow the number of allow-
able solutions and in particular to specify the depth
of the upper edge of the anomalous body.

The final step of the investigation is the geological
and geophysical generalization where those models
which best fit the geological and geophysical data
are selected from the results of the geoelectric meth-
ods.

### 5.2. The possibilities of the MVP

To assess the problems of MVP interpretation we
shall formulate the possibilites of the method:

(1) The observation of the geomagnetic variation
anomalous behavior in the local region allows a reli-
able conclusion to be made about the existence of the
electrical-conductivity anomaly.

(2) According to the extreme positions of the hori-
zontal components of the anomalous field or according
to the sign change of the vertical field we can localize
the epicentral line of the anomalous body and deter-
mine its strike. This may be performed by induction-
vector plotting. However, one should bear in mind
the possibility of axis displacement due to regional
background in the vertical component.

(3) The form of the profile curves of the anomalous
field makes it possible to determine $h_{max}$, the maxi-
mum depth to the upper edge of the conducting body
and $L_{x,max}$, its maximum effective width. Two oppo-
site models are used to estimate these two values:
one with a concentrated source (buried linear current)
and the other with a thin inhomogeneous surface
layer. If the profile curve is sufficiently simple, it is
possible to determine from its typical points the depth

of linear current which estimates $h_{max}$. In the case of a curve of complex shape it is possible to determine $h_{max}$ by determining the poles of the corresponding analytical function using the analytical continuation method.

(4) At central and long periods the frequency dependence of the MVP anomalous field makes it possible to give maximum and minimum estimations of the longitudinal conductivity $G = \sigma_i Q$ of the anomalous body with section $Q$ and to give minimum values for the body length $L_y$. The estimation technique is based on the results presented in Sections 3 and 4. The minimum estimate $G$ is the most interesting and objective one. It proceeds from two assumptions: (1) the anomaly is two-dimensional; and (2) the anomalous field is of conductive nature. When one or both assumptions are invalid the value of real $G$ is underestimated and the estimation is called the minimum one.

## 6. The estimation of $G_{min}$

The main method for estimating $G_{min}$ is based on the transformation of $h_z(T)$ $(r = x,z)$ into a function $V(T)$ by dividing by the normal impedance $\zeta_0$ and damping function $\beta$ according to formula (6) or (4). Thus the information on the normal geoelectrical section which complicates the frequency dependence is removed.

The obtained $V(T)$ is compared to theoretical values of (Fig. 1D or 2B, according to the type of model chosen) $V(\lambda/a)$ and $G_{min}$ is determined from the horizontal displacement of the $x$ axes. For stable $G_{min}$ determination it is sufficient to know the order of $\sigma_i/\sigma_e$ and the ratio of the maximum size of the body section to its minimum must not exceed 10. If the latter condition is not satisfied the $G_{min}$ value may be further underestimated.

A simplified way to estimate $G_{min}$ uses the empirical relation for the typical point position of the frequency curve, e.g. $T_0$ with $G_{min}$. Such a relation can be constructed from the synthesized frequency dependences of the anomalous field for the insertion and cylinders and may be described by the empirical formula:

$$G_{min} [\Omega^{-1} \text{ m}] = 5 \cdot 10^4 \{T_0 [\text{sec}]\}^{1.2} \qquad (8)$$

A third more approximate way is to use the profile curve of the anomalous field at one period. The zero moment of the anomalous field is defined by the expressions (Rokityansky and Shuman, 1971; Rokityansky, 1972):

$$m_0 = \frac{1}{4\pi^2} V\beta\zeta_0 G; \qquad m_0 = -\frac{1}{2\pi} \int\limits_{-\infty}^{\infty} h_x(x)dx \qquad (9)$$

The latter expression makes it possible to calculate $m_0$ from the observed field and the former one allows $G$ to be found when $V, \beta, \zeta_0$ are known. To find $G_{min}$ it is possible to use the inequality $|V\beta| \leqslant 1$.

## 7. The application of the frequency dependence method to the coastal-effect analysis

The original data are taken from the works by Sasai (1969), Cochrane and Hyndman (1970) and Schmucker (1970) where the amplitudes and phases of the anomalous fields are given for periods 15, 30, 60 and 120 min at a number of points on the Pacific coasts of North America and Japan. The combined data analysis of amplitudes and phases allows the determination of the position of $T_0$, the maximum of the amplitude dependence, and the sign change of the phase. Five stations are chosen for the investigation of frequency dependence of the coastal effect. The sea-bottom profile across these stations is quite smooth and the average depth $h$ of the adjacent sea (ignoring the shelf) varies from 4 to 1 km for the different stations. The analysis showed that the position of the maximum of the frequency dependence $T_0$ is associated with the adjacent sea depth $h$ by the approximate empirical formula $T_0 [\text{sec}] = 250 (h [\text{km}])^{1.7}$. The longitudinal conductivity $G$ of the sea section where the anomalous currents effectively flow at period $T_0$ is defined according to formula (8). Since $\sigma_i$ of the sea and $h$ are known we can find the sea band-width $L_0$ where the anomalous currents responsible for the coastal-effect flow. In the investigated range $h = 1-4$ km the value $L_0$ was approximately constant and was of average value $8h$ (with allowance for possible error of the result $5-13$).

The source parameter for the coastal effect therefore becomes known and is the current band $L_0$ $\simeq 8h$ at period $T_0$. With changing period the band

width may be approximated from the skin-effect laws. The small width of the coastal-effect source (several tens of km) allows it to be classified as a local anomaly of a quasi-conductive type (it is proportional to the normal impedance, but the function $V$ does not approach an asymptote with increasing $T$).

Observation of the frequency dependence of the coastal effect along a profile makes it possible to determine the electrical properties of the earth's crust and the upper-mantle edge on this profile. In this, the coastal concentration of the electric currents in the sea is used as a source.

Thus definite frequency dependence of the anomalous field arising from the coastal effect corresponds to each sea depth: $T_0 = 40$ min corresponds to the depth 4 km; 4 min to 1 km; and 15 sec to 200 m. These figures explain why the shelf does not produce the . coastal effect in bay-like magnetic variations, whereas the induction vectors, constructed from variations with periods of tens of minutes indicate the deep-sea parts. These figures explain all data obtained for the coastal effect in four profiles in North America and one profile of Japan by currents in the sea without any suggestion about the uplift of the mantle matter of high conductivity under the ocean. If the uplift of the conducting basement under the ocean exists and causes the greater part of the coastal effect, the maximum of the anomalous field frequency dependence would be longer periods because of the very high total longitudinal conductivity that is inevitable with the conductor of great thickness. A sharp decrease of the coastal effect with daily variations as compared to the bay variations is at variance with the suggestion that the mantle is the source of the coastal effect. On the other hand a high anomalous field at nearly 24-h periods confirms a mantle nature of the conductivity anomaly.

The data obtained for the coastal-effect parameters aids the investigation of the complicated situations when the observed fields are due to the coastal effect-superposition on the crustal anomaly effect (Japan, Peru—Bolivia and others).

## 8. Conclusion

The interpretation technique presented is applicable to two-dimensional anomalies when the direc-

tion $x$ exists along which eq. 1 is realized with satisfactory approximation. If the horizontal and vertical components of the anomalous field do not correspond at all to each other on the profile in the sense of eq. 1 (such an anomaly is observed in the western part of the Ukrainian shield) this is the case where array studies should be conducted. Array studies are also required when the field inhomogeneity of the original source is to be taken into account or is to be investigated.

Generally, array studies are always desirable if possible. It is also reasonable to apply classical methods of processing and interpretation to the array study data obtained, including induction-vector plotting and transfer-function determination over a wide range of periods in order to obtain the anomalous field frequency dependence. For a detailed determination of the form of the profile curve necessary to estimate the maximum possible depth of the anomalous body additional detailed field work in the region of the anomaly is required. The final stage of electrical conductivity investigation is to carry out MTS or deep electrical sounding with other methods over the anomalous body in order to determine the real depth to its upper edge.

## References

Banks, R.I., 1973, Phys. Earth Planet. Inter., 7: 339.
Cochrane, N.A. and Hyndman, R.D., 1970. Can. J. Earth Sci., 7: 1208–1218.
Dmitriev, V.I. and Kokotushkin, G.A., 1971. The Master Curves for the Magneto-telluric Sounding in Inhomogeneous Media. Moscow State University, Moscow.
Dmitriev, V.I., Zakharow, E.V. and Kokotushkin, G.A., 1973. The Master Curves for the Magnetotelluric Sounding in Inhomogeneous Media. Moscow State University, Moscow.
Kaufman, A.A., 1960, Izv. High Schools, Ser. Geol. Geophys., No. 6.
Kaufman, A.A., Tabarovsky, L.A. and Terentiev, S.A., 1971a. The Electromagnetic Field of the Plane Wave in the Medium Enclosing Elliptical Cylinder ($E$-polarization). Novosybirsk.

Kaufman, A.A., Tabarovsky, L.A. and Terentiev, S.A., 1971b.
    The Electromagnetic Field of the Elliptical Cylinder in a
    Horizontal Stratified Medium. Novosybirsk.
Kertz, W., 1954. Nachr. Akad. Wiss. Göttingen, Math. Phys.,
    Kl. 2A, pp. 101–110.
Rokityansky, I.I., 1972. Geophysical Methods of the
    Magneto-Variation Sounding and Profiling. Naukova dumka
    Kiev.
Rokityansky, I.I., 1974. Geofiz. Sb., Akad. Nauk Ukr. S.S.R.,
    58: 65.
Rokityansky, I.I. and Kulick, S.N., 1972. Geofiz. Sb., Akad.
    Nauk Ukr. S.S.R., 47: 71.
Rokityansky, I.I. and Shuman, V.N., 1970. Izv. Akad. Nauk
    S.S.S.R., Ser. Fiz. Zemli (Ser. Phys. Earth), 10: 39.

Rokityansky, I.I. and Shuman, V.N., 1971. Izv. Akad. Nauk
    S.S.S.R., Ser. Fiz. Zemli (Ser. Phys. Earth), 8: 63.
Rokityansky, I.I., Logvinov, I.M. and Luginina, N.A., 1969.
    Izv. Akad. Nauk S.S.S.R., Ser. Fiz. Zemli (Ser. Phys. Earth),
    3: 100.
Sasai, Y., 1969. Geomagnetic variation anomaly in the central
    part of Japan. Proc. Symp. on Conductivity Anomaly,
    Earthquake Res. Inst., Univ. Tokyo, 2: 43–55.
Schmucker, U., 1970. Bull. Scripps Inst. Oceanogr., 13: 165.
Svetov, B.S. et al., 1966. Prospecting Electromagnetic Methods
    in Ore Geophysics. Nedra. Moscow.
Svetov, B.S., 1973. The Theory, Methods and Interpretation of
    the Materials of the Low Frequency Inductive Electrical
    Prospecting. Nedra, Moscow.